

Wireless Communication Based on Microwave Photon-Level Detection With Superconducting Devices: Achievable Rate Prediction

Junyu Zhang, Chen Gong, Shangbin Li, Rui Ni, Chengjie Zuo, Jinkang Zhu, Ming Zhao, and Zhengyuan Xu

Abstract—Future wireless communication system embraces physical-layer signal detection with high sensitivity, especially in the microwave photon level. Currently, the receiver primarily adopts the signal detection based on semi-conductor devices for signal detection, while this paper introduces high-sensitivity photon-level microwave detection based on superconducting structure. We first overview existing works on the photon-level communication in the optical spectrum as well as the microwave photon-level sensing based on superconducting structure in both theoretical and experimental perspectives, including microwave detection circuit model based on Josephson junction, microwave photon counter based on Josephson junction, and two reconstruction approaches under background noise. In addition, we characterize channel modeling based on two different microwave photon detection approaches, including the absorption barrier and the dual-path Handury Brown-Twiss (HBT) experiments, and predict the corresponding achievable rates. According to the performance prediction, it is seen that the microwave photon-level signal detection can increase the receiver sensitivity compared with the state-of-the-art standardized communication system with waveform signal reception, with gain over 10dB.

Key Words: Microwave photon detection, Josephson junction, Superconducting absorption barrier, Handury Brown-Twiss (HBT) experiments.

I. INTRODUCTION

With the development of future wireless communication system, the Internet of Things (IoT) technology that constitutes the Internet of Everything is promising for both industrial and daily applications. Thus, reducing the energy consumption of narrowband communication is attracting extensive interests from both academia and industrial areas. One key challenge is the signal detection under extremely weak power regime. Due to wave-particle duality of the electromagnetic field, the microwave waveform degrades into microwave photons under the extremely weak electromagnetic power. The signal detection need resort to the approach based on the microwave photon processing.

This work was supported by National Key Research and Development Program of China (Grant No. 2018YFB1801904), Key Program of National Natural Science Foundation of China (Grant No. 61631018), Key Research Program of Frontier Sciences of CAS (Grant No. QYZDY-SSW-JSC003). Junyu Zhang, Chen Gong, Shangbin Li, Chengjie Zuo, Jinkang Zhu, Ming Zhao, and Zhengyuan Xu are with Key Laboratory of Wireless-Optical Communications, Chinese Academy of Sciences, School of Information Science and Technology, University of Science and Technology of China, Hefei, China. Email: jy970102@mail.ustc.edu.cn, {cgong821,shbli, czuo, jkzhu, zhaoming_xuzu}@ustc.edu.cn.

Rui Ni is with Huawei Technology, Shenzhen, China. Email: raney.nirui@huawei.com.

On the other hand, in optical spectrum, photon-level detection can be accomplished using the photoelectric effect, where the energy of a single photon is high enough to excite detectable electrons in room temperature. In microwave frequencies, the energy of a single microwave photon is lower to a magnitude of five orders, which increases the difficulties of photon-level detection, especially at room temperature with strong ambient radiation. Conventional detection adopts non-linear resistive components, typically Schottky barrier diodes as rectifiers and heterodyne mixers. The sensitivity of such mixer typically lies in the waveform power regime [1].

In order to realize microwave photon-level detection in the microwave frequency band, it is necessary to reduce the background temperature such that the single photon energy is differentiable in the ambient radiation. The superconducting structure in low temperature serves as a good candidate for the receiver device, where electron-phonon interactions lead to weak gravitational forces between electrons. In some materials, at sufficiently low temperatures, such weak gravitational force can lead to a binding pair, i.e., a superconducting ground state. Single-element excitation above this ground state requires a minimum threshold energy and consists of quasi-particles with both electrons and holes. Cohen, Falicov, and Phillips proposed the Hamiltonian theory to characterize the potential barrier between quasi-particle tunneling between two volume superconductors [2]. After that, Josephson made an significant prediction that the superconducting pair could also pass through the barrier tunnel and derived the consequences of the Josephson Tunnel using the same Hamiltonian model. The Josephson junction consists of two weakly connected superconductors, such that a pair of currents can only be generated on both sides of the Josephson junction by tunneling through a weak barrier. [1] A typical model of the Josephson junction is a superconducting-insulator-superconductor (SIS) interlayer.

When the quantum voltage at the incident frequency exceeds the voltage width of the quasi-particle tunneling threshold, the SIS responds to a single quantum through a photon-assisted tunneling mechanism. This allows the SIS junction to perform microwave/millimeter wave photon detection close to the quantum limit [3]–[6]. Besides, a single microwave photon can also be detected by microwave-mechanical-optical coupling [7]–[12] or nitrogen-vacancy center [13], [14], but the superconducting method still has the advantages of high sensitivity and standardized manufacturing process.

The strong interaction of superconducting integrated circuits

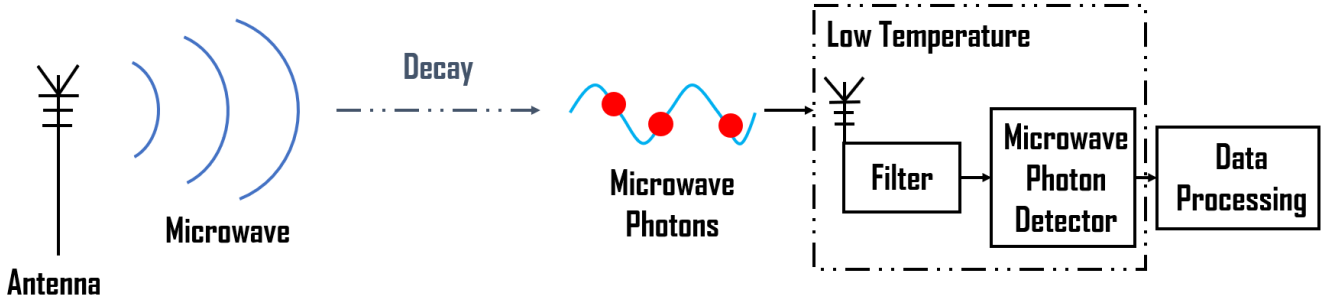


Fig. 1. System architecture of wireless communication transmission based on quantized microwave photon-level detection.

with microwave photons forms the basis of circuit quantum electrodynamics (cQED). An efficient and versatile microwave photon counter can be realized based on microwave-induced transitions between discrete energy levels in the Josephson junction [15]. Utilizing more efficient counter and microwave photon detection element [16], we can perform various types of experiments and measurements, including Bell's inequality experiments, all quantum based on optics and measurement, quantum computation, quantum homodyne tomography, and quantum communication and cryptography [17], [18]. These are essential for quantum information processing and communication [19].

Particularly in superconducting circuits, photoelectric conversion can be accomplished by the coupling of optical and microwave fields using micromechanical resonators [20], where the microwave radiation collected from the target area is phase conjugated and upconverted into a light field. Such kind of microwave quantum illumination system or quantum radar outperforms conventional microwave radar [21].

In this paper, we firstly propose the concept of quantized signal reception architecture based on superconducting devices. Then, we overview existing theoretical and experimental works on photon-level microwave signal reception. We predict the achievable transmission rates for two types of superconducting structure, based on absorption barrier and two-path Handury Brown-Twiss (HBT) experiments. It is predicted that compared with the state-of-the-art communication standard, the proposed approach can outperform via over 10dB.

The remainder of this work is organized as follows. In Section II, we outline the system architecture with superconducting signal reception device. In Section III, we overview the existing works on the superconducting structure based signal reception. In Section IV, we analyze the achievable rate based on absorption barrier. In Section V, we analyze the achievable rate based on two-path signal measurement. Finally, concluding remarks are given in Section VI.

II. SYSTEM ARCHITECTURE

In this section, we propose a system architecture for wireless communication based on quantized microwave photon-level detection with superconducting devices, as shown in Figure 1.

The transmitting antenna sends the modulated signal, which suffers strong attenuation during the transmission in the space.

According to the wave-particle duality, the microwave signal exhibits a particle image, which calls for quantized microwave photon-level signal detection. At the receiver side, we adopt a microwave photon-level detector based on superconducting devices for signal reception, and perform data processing based on its output signal. A narrowband filter is adopted ahead of the photon-level detector to reduce the interference in the neighborhood spectrum.

III. REVIEW OF EXISTING WORKS

We overview existing works and basic principles on photon-level detection in the optical spectrum, as well as the microwave photon-level signal detection, including microwave photon counters based on superconducting structures and the reconstruction of quantum states in a noisy environment.

A. Photon-level Communication System in the Optical Spectrum

The photon-level signal detection-based communication system design has been extensively studied for optical communication. Within a fixed time period, the number of detected photons conforms to the following Poisson distribution,

$$P(N = n) = \frac{\bar{\lambda}^n}{n!} e^{-\bar{\lambda}}, \quad (1)$$

where the mean number $\bar{\lambda}$ can be obtained from the received signal energy within that period divided by the energy per photon. The achievable communication rate and signal detection can be performed based on the Poisson distributed number of photons.

For such types of channels, it can be proved that on-off keying (OOK) modulation with sufficiently short symbol interval can approach the capacity [22]–[24]. More specifically, letting λ_s and λ_b denote the mean photon numbers of the signal and noise components, respectively, the mean numbers of photons corresponding to symbols one and zero are $\lambda_s + \lambda_b$ and λ_b , respectively. The signal detection performance can be analyzed based on the following two Poisson distributions for symbol zero and symbol one,

$$P(n|\text{zero}) = \frac{\lambda_b^n}{n!} e^{-\lambda_b}, \quad (2)$$

$$P(n|\text{one}) = \frac{(\lambda_s + \lambda_b)^n}{n!} e^{-(\lambda_s + \lambda_b)}. \quad (3)$$

In the atmosphere, the above photon-level signal model can well characterize the non-line-of-sight(NLOS) ultraviolet scattering communication, where large path loss of the NLOS link leads to photon-level signal intensity and negligible background radiation can guarantee the photon-level signal sensitivity. The inter-symbol interference structure due to the finite bandwidth transmitter device is investigated in [25]. To expand the transmission range, the multi-hop relay communication has been investigated in [26], [27].

Under a turbulence channel, the received signal exhibits a doubly stochastic characteristic due to both signal intensity variation and Poisson distributed photons given fixed signal intensity. Such type of channel can be characterized by a hidden Markov chain model, where the hidden state represents the strength of the received signal, and the observation represents the number of photons given the hidden state. Assume that there are K states in the mixed Poisson signal model. The received signal can be characterized by the following mixed Poisson model,

$$P(N = n) = \sum_{k=1}^K p_k \frac{\lambda_k^n}{n!} e^{-\lambda_k}, \quad (4)$$

where p_k and λ_k denote the probability and mean number of photons corresponding to state k , respectively. The related parameters of the probability distribution can be estimated via expectation-maximization(EM) algorithm [28].

Due to the finite bandwidth of the receiver detector, the output pulse of each photon exhibits positive rising edge and falling edge. Such phenomenon causes positive dead time, leading to the mergence of the two pulses if the incidence time between the two photons is shorter than the dead time. The received signal statistics and symbol detection are characterized in [29].

For the photon-level communication system realization, the receiver performs counting-based signal synchronization, Poisson distribution-based signal detection and channel code decoding. More details on the system realization and experiments can be found in [30].

B. Microwave Photon Counter Based on Josephson Junction

According to [19], as the bias current of Josephson junction approaches a critical value I_0 , the potential of the junction approaches the local minimum, which consists of a few discrete energy levels. The resonance of receiving a microwave photon produces an oscillation between ground state $|0\rangle$ and excited state $|1\rangle$ of the Josephson junction, which tunnels to a continuous state at rates Γ_0 and Γ_1 , respectively. Since the tunneling rate depends on the barrier height, Γ_1 tends to be 2-3 orders of magnitude larger than Γ_0 , as shown in Figure 2. Due to different tunneling rates for the two states, a microwave photon-counter can be designed.

Based on this principle, the direct-current (DC) operating point of the microwave counter is set to be close to the critical current of Josephson junction. The peripheral circuit of the Josephson junction can almost resonate with the incident microwave photon, causing the transition from ground state $|0\rangle$ to excited state $|1\rangle$. The Josephson junction in the excite

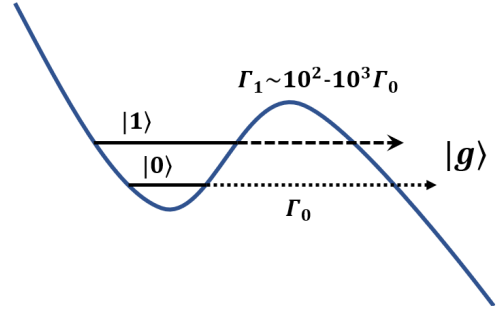


Fig. 2. Junction potential energy landscape.

state has a faster tunneling rate than the ground state, leading to a large pulse, and the comparator tends to output a count. The schematic diagram of the circuit is shown in Figure 3.

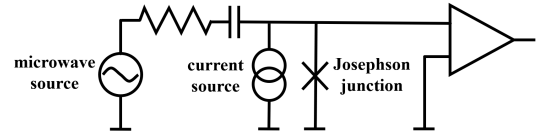


Fig. 3. Schematic diagram of the circuit.

To check the performance of the counter, we define its efficiency

$$\eta \equiv P_{\text{bright}}(1 - P_{\text{dark}}), \quad (5)$$

where P_{bright} denotes the probability that the comparator can correctly generate the count after the incidence of the microwave counter; and P_{dark} denotes the probability that the Josephson junction generates a count under no microwave incidence.

It is reported that such efficiency can reach 0.7 and can be kept above 0.6 in a 450 MHz wide frequency band [19].

C. A Microwave Photon Counter Based on a Discrete Superconducting Structure

A microwave photon counter based on discrete superconducting structure employs metamaterial that realizes single-wave photon detection through irreversible absorption of microwave photons [31]. When a microwave photon enters the device, it is captured with a certain probability. Then, the system reaches a stable state that can be observed mesoscopically after the absorption process. More specifically, the microwave photon counter consists of a set of photon absorbers placed along an one-dimensional waveguide, which can be constructed with a bi-stable quantum circuit similar to that used to implement the qubit. These circuits are capable of capturing photons and transitioning from initial state $|0\rangle$ to steady state $|g\rangle$.

In the counting process, the counting is done after the absorption process. The detection process is thus passive and does not require any extra control. Numerical results show that as the number of photon absorbers increases, the entire photon absorption/detection probability can reach 90% [31].

D. Microwave Quantum State Reconstruction in Noisy Environment

For microwave communication based on photon-level detection, information can be detected through the quantum states at the receiver, which inevitably suffers noise and needs to be reconstructed based on statistical methods.

1) *Conjugate Orthogonal Component Quantum State Reconstruction*: Consider the quantum states of field mode a , which can be reconstructed using infinite set of moments $\langle (a^\dagger)^n a^m \rangle$ for $m, n \geq 0$. The mark '†' stands for Hermitian conjugate. Moreover, it can be approximated by finite terms via limiting the size of $n + m$ [32].

Assume that a is amplified by a linear amplifier with factor G , which introduces noise h . The amplified signal is mixed with in-phase and out-of-phase local oscillators in the mixer to perform frequency-down processing to detect a set of conjugate orthogonal components \hat{X} and \hat{P} , given by

$$\sqrt{G}(\hat{X} + i\hat{P}) = \sqrt{G}(a + h^\dagger) \equiv \hat{S}. \quad (6)$$

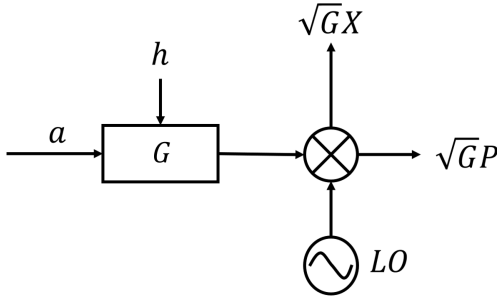


Fig. 4. Generation of orthogonal components \hat{X} and \hat{P} .

Noise h can be well approximated as a Gaussian phase space distribution. Besides, the measured distribution of \hat{S} at the output is

$$D^{[\rho]}(S) = \frac{1}{G} \int d^2\beta P_a(\beta) Q_h\left(\frac{S^*}{\sqrt{G}} - \beta^*\right), \quad (7)$$

where P_a is the Glauber-Sudarshan P function of mode a and Q_h is the Husimi Q function of noise h [33]–[35]. Figure 4 shows the process of obtaining the amplified expectations of two orthogonal components \hat{X} and \hat{P} from the input signal. In particular, for vacuum state $|0\rangle$, $P_a(\beta) = \delta^{(2)}(\beta)$, and thus

$$D^{[|0\rangle\langle 0|]}(S) = \frac{1}{G} Q_h\left(\frac{S^*}{\sqrt{G}}\right). \quad (8)$$

The second state $|\psi\rangle$ in the signal detection can be selected as the state of interest, such as Fock state $|1\rangle$. Then, we can get $D^{[|\psi\rangle\langle\psi|]}$ by measurement, and thus

$$\langle (\hat{S}^\dagger)^n \hat{S}^m \rangle_\rho = \int d^2S (S^*)^n S^m D^{[\rho]}(S). \quad (9)$$

When the signal and noise are not correlated, we have

$$\begin{aligned} \langle (\hat{S}^\dagger)^n \hat{S}^m \rangle_\rho &= G^{(n+m)/2} \sum_{i,j=0}^{n,m} C_m^j C_n^i \langle (a^\dagger)^i a^j \rangle \\ &\times \langle h^{n-i} (h^\dagger)^{m-j} \rangle. \end{aligned} \quad (10)$$

More specifically, for a vacuum state, we have

$$\langle (\hat{S}^\dagger)^n \hat{S}^m \rangle_{|0\rangle\langle 0|} = G^{(n+m)/2} \langle h^{n-i} (h^\dagger)^{m-j} \rangle. \quad (11)$$

Based on $\langle (\hat{S}^\dagger)^n \hat{S}^m \rangle_\rho$ and $\langle (\hat{S}^\dagger)^n \hat{S}^m \rangle_{|0\rangle\langle 0|}$, we can get $\langle (a^\dagger)^n a^m \rangle$, such that the quantum state reconstruction can be completed. Based on $\langle (a^\dagger)^n a^m \rangle$, we can restore the information on the quantum state, e.g., the following Winger function of state S ,

$$W(\alpha) = \sum_{n,m} \int d^2\lambda \frac{\langle (a^\dagger)^n a^m \rangle (-\lambda^*)^m \lambda^n}{\pi^2 n! m!} e^{-\frac{1}{2}|\lambda|^2 + \alpha\lambda^* - \alpha\lambda^*\lambda}. \quad (12)$$

2) *Dual Signal Reconstruction Scheme*: A two-way reconstruction scheme that obtains the statistics $\langle S^n \rangle$ of signal S is reported in [36]. Assuming signal $S\sqrt{2}$ is equally separated by a four-port 50-50 microwave beam splitter, which are amplified via G with noise components χ_1 and χ_2 . The output signals, denoted as C_1 and C_2 , are given by

$$\begin{aligned} C_1 &= G(S + V + \chi_1), \\ C_2 &= G(-S + V + \chi_2), \end{aligned} \quad (13)$$

where V is an additional signal artificially introduced from

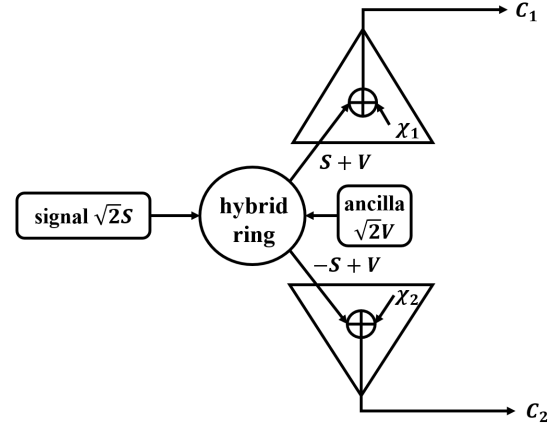


Fig. 5. Dual signal model.

the four-port beam splitter, assuming that the information of V is completely known. Figure 5 shows the process from the input signal to dual signal. It is assumed that $\langle \chi_1 \rangle = \langle \chi_2 \rangle = 0$, $\langle V^{2j+1} \rangle = 0$, and that the value of $\langle C_1^i C_2^m \rangle$ can be obtained by measurement, such that the statistics of signal S and noise χ can be obtained. Then, we have that

$$\begin{aligned} \langle S^n \rangle &= \langle C_1^{n-1} C_2 \rangle / G^n \\ &- \sum_{k=1}^{n-1} \sum_{j=0}^k C_{n-1}^k C_k^j \langle S^{n-k} \rangle \langle V^j \rangle \langle \chi_1^{k-j} \rangle \\ &+ \sum_{k=0}^{n-1} \sum_{j=0}^k C_{n-1}^k C_k^j \langle S^{n-k-1} \rangle \langle V^{j+1} \rangle \langle \chi_1^{k-j} \rangle \end{aligned} \quad (14)$$

$$\begin{aligned} \langle \chi_1^n \rangle &= \langle C_1^n \rangle / G^n \\ &- \sum_{k=1}^n \sum_{j=0}^k C_n^k C_k^j \langle \chi_1^{n-k} \rangle \langle S^{k-j} \rangle \langle V^j \rangle, \end{aligned} \quad (15)$$

$$\langle \chi_2^n \rangle = + \langle C_2^n \rangle / G^n - \sum_{k=1}^n \sum_{j=0}^k C_n^k C_k^j (-1)^{k-j} \langle \chi_2^{n-k} \rangle \langle S^{k-j} \rangle \langle V^j \rangle. \quad (16)$$

It can be seen that the signal statistics can be obtained by a recursive method. The central moment can be obtained from:

$$\langle (S - \langle S \rangle)^n \rangle = \sum_{k=0}^n C_n^k (-1)^{n-k} \langle S^k \rangle \langle S \rangle^{n-k}. \quad (17)$$

IV. MICROWAVE PHOTON DETECTION BASED ON SUPERCONDUCTING ABSORBING BARRIER

We elaborate the model of superconducting absorption barrier [31], outline the communication system model, and numerically evaluate the achievable rate.

A. Superconducting Absorption Barrier [31]

The superconducting absorption barrier consists of a set of microwave photon absorbers coupled by a one-dimensional waveguide [31], which can be realized by a Josephson junction at a critical current bias and is able to capture and count the microwave photons.

When the Josephson junction is close to the critical current bias, the local minimum of potential consists of discrete energy levels, such as the ground state $|0\rangle$ and excite state $|1\rangle$. States $|0\rangle$ and $|1\rangle$ transition to the continuous state $|g\rangle$ at the rates of Γ_0 and Γ , respectively, where $\Gamma \gg \Gamma_0$.

The Hamiltonian H contains the absorber and radiation field, as well as wave functions ψ_l and ψ_r propagating in the left and right directions at group velocity v_g , respectively. The interaction between the two wave functions is established by the delta potential field of intensity V , given by

$$H = \sum_i \hbar\omega |1\rangle_i \langle 1| + i\hbar v_g \int dx S_{lr} + \sum_i \int dx V \delta(x - x_i) [\psi_{lr} |1\rangle_i \langle 0| + H.c.], \quad (18)$$

where $S_{lr} = \psi_l^\dagger \partial_x \psi_l - \psi_r^\dagger \partial_x \psi_r$, $\psi_{lr} = \psi_l + \psi_r$, x_i and $|0\rangle_i$, $|1\rangle_i$ are the position and states of the i^{th} absorber, respectively.

The density matrix of the waveguide and absorber is characterized by

$$\frac{\partial \rho}{\partial t} = -\frac{i}{\hbar} [H, \rho] + \mathcal{L}\rho, \quad (19)$$

where $\mathcal{L} = \sum_i \mathcal{L}_i$; and \mathcal{L}_i represents the standard attenuation term for each absorbed microwave photon i , given by

$$\mathcal{L}_i \rho = \frac{\Gamma}{2} (2|g\rangle_i \langle 1| \rho |1\rangle_i \langle g| - |1\rangle_i \langle 1| \rho - \rho |1\rangle_i \langle 1|). \quad (20)$$

For each absorber j , the quantum state transition can be characterized by the incident intensity, reflection $|r|^2$, and transmission intensity $|t|^2$, given by the following scattering matrix \mathbf{T}_j ,

$$\mathbf{T}_j = \begin{pmatrix} 1 - 1/\gamma & -1/\gamma \\ 1/\gamma & 1 + 1/\gamma \end{pmatrix}, \quad (21)$$

where $\gamma = (\Gamma - \sqrt{-1}\delta)v_g/V^2$, $\delta = \omega - \omega_\mu$, and ω_μ is the characteristic frequency of the absorber. For each absorber, absorption is equivalent to microwave photons that are not reflected or transmitted, such that the absorption rate of a single absorber is given by

$$\alpha = 1 - \frac{1 + |T_{01}|^2}{|T_{11}|^2} = \frac{2\gamma}{(1 + \gamma)^2}. \quad (22)$$

It can be seen that the absorption probability of a single absorber is at most 0.5, while the absorption rate of the whole system can be increased by adopting multiple absorbers. Via increasing the number of absorbers N and optimizing parameter γ , the absorption probability above 90% can be achieved, as shown in Figure 6.

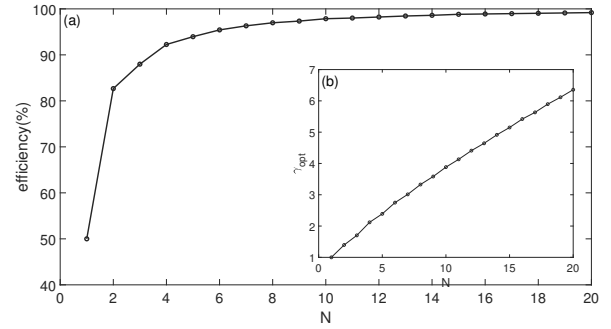


Fig. 6. (a) The relationship between the optimal absorption efficiency and the number N of absorbers, (b) The relationship between the optimal parameter values and the number N of absorbers.

For real circuit, assume that the capacitance of Josephson junction is C_j , the gate capacitance of the Josephson junction frontend and the microwave coupling is C_g . Then, parameter γ can be expressed as

$$\gamma = \frac{\alpha^2}{c_{12}} \frac{\hbar}{eZ_0} \frac{\Gamma_1 - i(\omega - \omega_\mu)}{\omega_\mu}, \quad (23)$$

where $c_{12} = C_g / (C_g + C_j)$; $\alpha^2 = 4e^2 / C_j \hbar \omega$; Γ_1 is the rate at which $|1\rangle$ is converted to $|g\rangle$; and Z_0 is a constant.

B. Equivalent Poisson Channel Modeling

Refer to the system model shown in Figure 1. Consider time-varying transmission power from on-off keying (OOK) modulation at the transmitter side with peak power constraint. Due to strong channel attenuation in the communication link, the received signal exhibits discrete number of signal photons yielding time-varying Poisson distribution, where the mean number of photons per slot is λ_1 for symbol on, and the intensity of background photon is λ_0 .

For channels based on superconducting absorption barrier, assume that each photon is absorbed by the barriers independently with probability p . Thus, the entire system model is given by Figure 7.

Thus, we have $N(t) \sim \mathcal{P}((\lambda_1 + \lambda_0)\tau)$ and $N_p(t) \sim \mathcal{P}(p(\lambda_1 + \lambda_0)\tau)$, where $\mathcal{P}(\lambda)$ denotes Poisson distribution with mean λ . Due to random extraction property of Poisson distribution, the transmission system can be characterized in Figure 8.

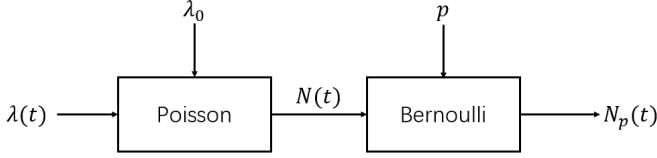


Fig. 7. Poisson channel with probability of reception.

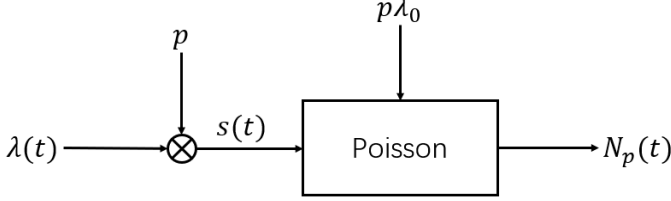


Fig. 8. The equivalent Poisson channel model.

For simplicity, we consider hard-decision based on the output signal. Let M denote the detection threshold, such that symbol one is detected if the number of detected photons exceeds M . Let

$$P_1 = \sum_{k=M}^{\infty} e^{-p(\lambda_1+\lambda_0)\tau} \frac{p^k (\lambda_1 + \lambda_0)^k}{k!}, \quad (24)$$

$$P_2 = \sum_{k=0}^{M-1} e^{-p\lambda_2\tau} \frac{p^k \lambda_2^k}{k!}. \quad (25)$$

Assume that symbol one is transmitted with probability γ , i.e., $P(X=1) = \gamma$ and $P(X=0) = 1 - \gamma$. We have the following conditional probability,

$$\begin{aligned} P(Y=1|X=1) &= P_1, P(Y=0|X=1) = 1 - P_1, \\ P(Y=1|X=0) &= P_2, P(Y=0|X=0) = 1 - P_2, \end{aligned} \quad (26)$$

where $P(Y=1) = \gamma P_1 + (1 - \gamma)(1 - P_2)$. For simplicity, we consider the following mutual information for the binary asymmetric channel,

$$I(X, Y) = H(P_\gamma) - \gamma H(P_1) - (1 - \gamma)H(P_2), \quad (27)$$

where function $H(x) = -x \log_2 x - (1-x) \log_2 (1-x)$. For the binary asymmetric channel under consideration, the optimal distribution on output Y is given by

$$P_\gamma^* = \frac{1}{1 + 2 \frac{H(P_1) - H(P_2)}{P_1 + P_2 - 1}}. \quad (28)$$

Moreover, higher achievable rate can be obtained via directly computing from the two Poisson distributions without hard decision between them.

C. Simulation Result

Assume that the single photon absorption probability is 0.9, and that the code rate is 1 kbps (symbol period 1ms). The carrier frequency of the transmitted microwave photon is 5GHz.

Assume that the antenna is placed at temperature T_A , such that the background radiation energy is given by kBT_A per slot; and the mean number of background photons per slot is $kBT_A/h\nu$. Assume that the signal reception power is P_r , such that the mean number of photons per unit time is $P_r/h\nu$.

The achievable rates are shown in Figure 9 for different temperatures T_A .

It can be seen that the achievable rate can reach above 0.95 for signal power -152dBm at room temperature 300K, and below -160dBm for temperature 50mK. Considering the LTE signal sensitivity of -100dBm with data rate 2.2Mbps, the power normalized to 1kHz bandwidth is between -130dBm and -135dBm also at room temperature [37]. It is seen that, the sensitivity gain of our proposed structure is over 20dB. Larger performance gain can be predicted via obtaining the achievable rate from two Poisson distributions without hard decision between them.

V. MICROWAVE PHOTON DETECTION BASED ON MICROWAVE HBT EXPERIMENT

We elaborate the output signal model of microwave HBT experiment [19], show the equivalent communication system statistics, and numerically investigate the achievable rate.

A. Microwave Hanbury Brown-Twiss Experiment [19]

In the microwave HBT experiment, the microwave photons emitted by the source are divided into two paths, which are detected by two microwave photon counters with relative delay. Both coherent microwave and thermal microwave are generated. The coherent microwave is generated by a microwave generator whose output is coupled to the detector through a transmission line with strong attenuation; and the thermal microwave is generated by amplifying, filtering, and upconverting the Johnson noise of the room temperature resistor. Double junction circuit is used to detect the statistics of the microwave photon source. Each junction has its own bias and readout. The schematic diagram of the experimental device is shown in Figure 10.

In the experiments, the output of two branches consists of two states, supercurrent state and voltage state, denoted as “0” and “1”, respectively. Let τ denote the relative delay between the two measurements in the two branches. Let $P_{00}(\tau)$, $P_{01}(\tau)$, $P_{10}(\tau)$ and $P_{11}(\tau)$ denote the probability that the two branches are in states “00”, “01”, “10” and “11”, respectively, for delay τ between the two branches. The values of $P_{00}(\tau)$, $P_{01}(\tau)$, $P_{10}(\tau)$ and $P_{11}(\tau)$ with respect to τ for coherent microwave and thermal microwave are shown in Figure 11. It is seen that for coherent microwave, the probabilities are constant for different delay; while for thermal microwave the probabilities vary with relative delay τ .

B. Equivalent SIMO Channel Modeling

Refer to the system model shown in Figure 1. Also assume OOK modulation and strong signal attenuation, such that the received signal cannot form continuous waveform. Within a symbol duration, the mean number of photons for symbol on is λ_1 , and the mean number of background radiation is λ_0 .

Assume that the signal paths are symmetrical, i.e., $P_{01}(\tau) = P_{10}(\tau)$. For coherent sources, we have $P_{11}^c(\tau) = p_c^2$, $P_{10}^c(\tau) = P_{01}^c(\tau) = p_c(1 - p_c)$, and $P_{00}^c(\tau) = (1 - p_c)^2$ for certain probability p_c ; and for thermal noise, we have $P_{11}^T(\tau) + P_{10}^T(\tau) = P_T$, $P_{10}^T(\tau) = P_{01}^T(\tau)$.

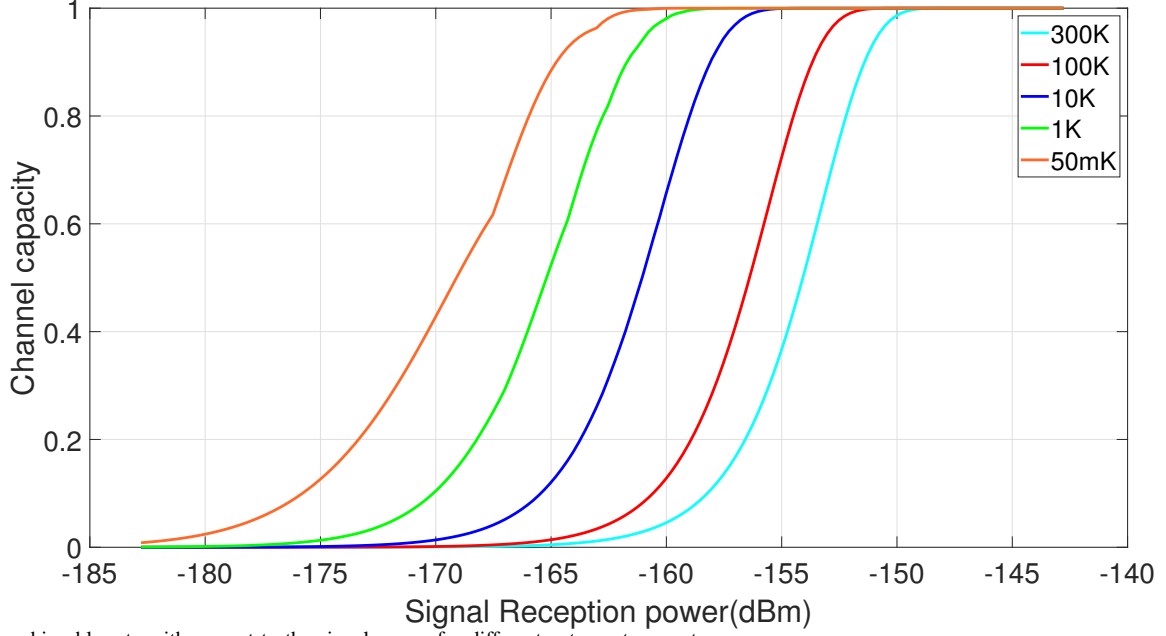


Fig. 9. The achievable rate with respect to the signal power for different antenna temperatures.

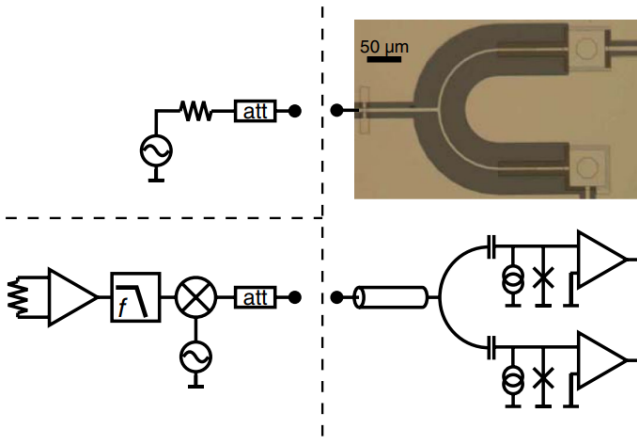


Fig. 10. The HBT experimental devices, where coherent microwave photon stream (upper left) and thermal noise microwave photon stream (bottom left) are divided into two-way counts (right side). [19]

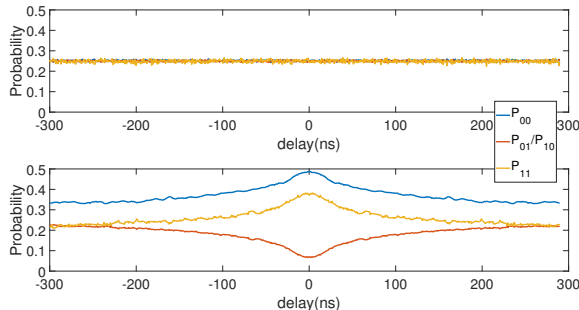


Fig. 11. The probability with respect to different delays for coherent microwave (top) and thermal microwave (bottom). [19]

Let N_{00}^c, N_{10}^c , and N_{01}^c denote the number of pulse combinations corresponding to states 00, 10, and 01, respectively; and the counterparts for thermal noise are given by N_{00}^T, N_{10}^T , and N_{01}^T , respectively.

The number of photons actually received for states 00, 10 and 01, denoted as N_{00}, N_{10} and N_{01} , respectively, are given by

$$\begin{aligned} N_{00} &= N_{00}^c + N_{00}^T, \\ N_{10} &= N_{10}^c + N_{10}^T, \\ N_{01} &= N_{01}^c + N_{01}^T. \end{aligned} \quad (29)$$

The channel model is shown in Figure 12. Now we give the following probability distribution at the receiving side, for symbols one and zero

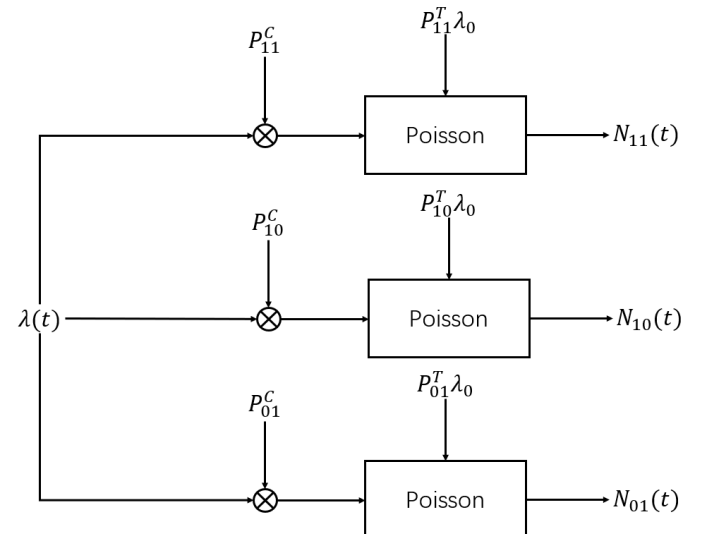


Fig. 12. The quantized microwave communication channel based on HBT experiment.

$$\begin{aligned}\Pi_1(k_{00}, k_{01}, k_{10}) &= p(N_{00} = k_{00}, N_{01} = k_{01}, N_{10} = k_{10}|1) \\ &= \prod_{i \in \{00, 01, 10\}} e^{-(P_i^C \lambda_1 + P_i^T \lambda_0)} \frac{(P_i^C \lambda_1 + P_i^T \lambda_0)^{k_i}}{k_i!},\end{aligned}\quad (30)$$

$$\begin{aligned}\Pi_0(k_{00}, k_{01}, k_{10}) &= p(N_{00} = k_{00}, N_{01} = k_{01}, N_{10} = k_{10}|0) \\ &= \prod_{i \in \{00, 01, 10\}} e^{-P_i^T \lambda_0} \frac{(P_i^T \lambda_0)^{k_i}}{k_i!}.\end{aligned}\quad (31)$$

Let p denote the prior distribution of symbol on. The achievable rate via OOK modulation is given by

$$\begin{aligned}C &= \max_{0 \leq p \leq 1} - \sum_{k_{00}, k_{01}, k_{10}} \Pi_p(k_{00}, k_{01}, k_{10}) \log \Pi_p(k_{00}, k_{01}, k_{10}) \\ &\quad - p \Pi_1(k_{00}, k_{01}, k_{10}) \log \Pi_1(k_{00}, k_{01}, k_{10}) \\ &\quad - (1-p) \Pi_0(k_{00}, k_{01}, k_{10}) \log \Pi_0(k_{00}, k_{01}, k_{10}),\end{aligned}\quad (32)$$

where $\Pi_p(k_{00}, k_{01}, k_{10}) = p \Pi_1(k_{00}, k_{01}, k_{10}) + (1-p) \Pi_0(k_{00}, k_{01}, k_{10})$. The second derivative of mutual information is

$$\frac{\partial^2 I}{\partial p^2} = - \sum \frac{(\Pi_1(k_{00}, k_{01}, k_{10}) - \Pi_0(k_{00}, k_{01}, k_{10}))^2}{\Pi_p(k_{00}, k_{01}, k_{10})} \leq 0, \quad (33)$$

The optimal prior probability p can be solved by convex optimization.

C. Channel Simulation

Assume that the symbol duration is 1ms, and that the coherent photon frequency $\nu = 3.8\text{GHz}$ [19]. We take typical coherent photon absorption probability $[P_{00}^C(\tau), P_{10}^C(\tau), P_{01}^C(\tau)] = [0.25 \ 0.25 \ 0.25]$, and thermal noise photon absorption probability $[P_{00}^T(\tau), P_{10}^T(\tau), P_{01}^T(\tau)] = [0.36 \ 0.07 \ 0.07]$. Other simulation configurations are the same as those in Section IV-C.

Assume that the antenna is placed at temperature T_A , such that the background radiation energy is given by kBT_A per slot; and the mean number of background photons per slot is $kBT_A/h\nu$. The achievable rates are shown in Figure 13 for different temperatures T_A .

It is seen that the achievable rate can reach above 0.95 for signal power -156dBm at room temperature 300K , and below -170dBm for temperature 50mK . From Section IV-C, the normalized power of LTE signal to 1kHz bandwidth is at room temperature is between -130dBm to -135dBm . Then, the performance gain of our proposed approach is over 15dB .

VI. CONCLUSION

We have envisaged a wireless communication system architecture based on microwave photon-level detection with superconducting devices. We have reviewed existing works on microwave photon sensing using superconducting structure, which can improve the receiver-side detection sensitivity compared with the state-of-the-art semi-conducting devices. We have also adopted two types of microwave photon detection methods based on microwave absorption barrier and HBT

experiments, characterized the corresponding communication channel models and predicted the achievable communication rate. It is seen that the microwave photon-level signal detection can improve the receiver sensitivity compared with the state-of-the-art communication system with waveform signal reception, with gain over 10dB . According to the performance prediction, our system can achieve significant performance improvement in low temperature environments. At present, commercial compact refrigerators can readily reduce the ambient temperature from 300K to below 10K within a few hours. So it is possible to deploy microwave photon-level detectors working in a low-temperature environment to increase the communication sensitivity.

In future work, we will focus on the coding based on the communication system architecture in Section II, and further communication performance improvement brought by more advanced superconducting devices. Moreover, conducting real experiments to evaluate the real communication system performance comprises of another major endeavor in the future.

REFERENCES

- [1] J. R. Tucker and M. J. Feldman, "Quantum detection at millimeter wavelengths," *Rev. Mod. Phys.*, vol. 57, pp. 1055–1113, 1985.
- [2] M. H. Cohen, L. M. Falicov, and J. C. Phillips, "Superconductive tunneling," *Phys. Rev. Lett.*, vol. 8, pp. 316–318, Apr 1962.
- [3] C. A. Mears, Q. Hu, P. L. Richards, A. H. Worsham, D. E. Prober, and A. V. Risnen, "Quantumlimited heterodyne detection of millimeter waves using superconducting tantalum tunnel junctions," *Applied Physics Letters*, vol. 57, no. 23, pp. 2487–2489, 1990.
- [4] P. L. Richards and Q. Hu, "Superconducting components for infrared and millimeter-wave receivers," *Proceedings of the IEEE*, vol. 77, no. 8, pp. 1233–1246, 1989.
- [5] M. J. Wengler, N. Dubash, G. Pance, and R. E. Miller, "Josephson effect gain and noise in SIS mixers," *IEEE Transactions on Microwave Theory and Techniques*, vol. 40, no. 5, pp. 820–826, 1992.
- [6] M. J. Wengler, "Submillimeter-wave detection with superconducting tunnel diodes," *Proceedings of the IEEE*, vol. 80, no. 11, pp. 1810–1826, 1992.
- [7] L. Midolo, A. Schliesser, and A. Fiore, "Nano-opto-electro-mechanical systems," *Nature Nanotechnology*, vol. 13, no. 1, pp. 11–18, 2018.
- [8] A. P. Higginbotham, P. S. Burns, M. D. Urmey, R. W. Peterson, N. S. Kampel, B. M. Brubaker, G. Smith, K. W. Lehnert, and C. A. Regal, "Harnessing electro-optic correlations in an efficient mechanical converter," *Nature Physics*, vol. 14, no. 10, pp. 1038–1042, 2018.
- [9] S. Barzanjeh, M. Abdi, G. J. Milburn, P. Tombesi, and D. Vitali, "Reversible optical-to-microwave quantum interface," *Phys. Rev. Lett.*, vol. 109, p. 130503, 2012.
- [10] K. Zhang, F. Bariani, Y. Dong, W. Zhang, and P. Meystre, "Proposal for an optomechanical microwave sensor at the subphoton level," *Phys. Rev. Lett.*, vol. 114, p. 113601, 2015.
- [11] O. c. v. Černotík, S. Mahmoodian, and K. Hammerer, "Spatially adiabatic frequency conversion in optoelectromechanical arrays," *Phys. Rev. Lett.*, vol. 121, p. 110506, 2018.
- [12] R. W. Andrews, R. W. Peterson, T. P. Purdy, K. Cicak, R. W. Simmonds, C. A. Regal, and K. W. Lehnert, "Bidirectional and efficient conversion between microwave and optical light," *Nature Physics*, vol. 10, pp. 321 EP –, Mar 2014.
- [13] T. Joas, A. M. Waeber, G. Braunbeck, and F. Reinhard, "Quantum sensing of weak radio-frequency signals by pulsed mollow absorption spectroscopy," *Nature Communications*, vol. 8, no. 1, p. 964, 2017.
- [14] B. Yang, Y. Dong, Z. Hu, G. Liu, Y. Wang, and G. Du, "Noninvasive imaging method of microwave near field based on solid-state quantum sensing," *IEEE Transactions on Microwave Theory and Techniques*, vol. 66, no. 5, pp. 2276–2283, 2018.
- [15] R. J. Schoelkopf, S. H. Moseley, C. M. Stahle, P. Wahlgren, and P. Delsing, "A concept for a submillimeter-wave single-photon counter," *IEEE Transactions on Applied Superconductivity*, vol. 9, no. 2, pp. 2935–2939, 1999.

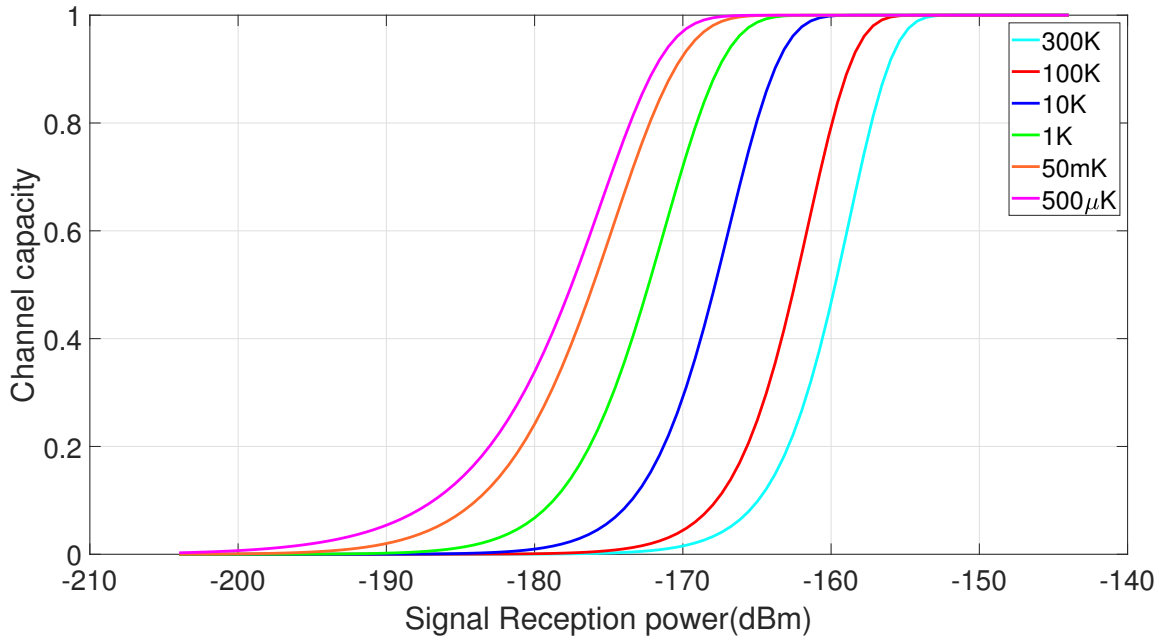


Fig. 13. The achievable rate with respect to the signal power for different antenna temperatures.

- [16] G. de Lange, B. van Heck, A. Bruno, D. J. van Woerkom, A. Geresdi, S. R. Plissard, E. P. A. M. Bakkers, A. R. Akhmerov, and L. DiCarlo, "Realization of microwave quantum circuits using hybrid superconducting-semiconducting nanowire josephson elements," *Phys. Rev. Lett.*, vol. 115, p. 127002, 2015.
- [17] N. Bergeal, F. Schackert, L. Frunzio, and M. H. Devoret, "Two-mode correlation of microwave quantum noise generated by parametric down-conversion," *Phys. Rev. Lett.*, vol. 108, p. 123902, 2012.
- [18] A. V. Semenov, I. A. Devyatov, P. J. de Visser, and T. M. Klapwijk, "Coherent excited states in superconductors due to a microwave field," *Phys. Rev. Lett.*, vol. 117, p. 047002, 2016.
- [19] Y.-F. Chen, D. Hover, S. Sendelbach, L. Maurer, S. T. Merkel, E. J. Pritchett, F. K. Wilhelm, and R. McDermott, "Microwave photon counter based on josephson junctions," *Phys. Rev. Lett.*, vol. 107, p. 217401, 2011.
- [20] S. Barzanjeh, M. Abdi, G. J. Milburn, P. Tombesi, and D. Vitali, "Reversible optical-to-microwave quantum interface," *Phys. Rev. Lett.*, vol. 109, p. 130503, 2012.
- [21] S. Barzanjeh, S. Guha, C. Weedbrook, D. Vitali, J. H. Shapiro, and S. Pirandola, "Microwave quantum illumination," *Phys. Rev. Lett.*, vol. 114, p. 080503, 2015.
- [22] A. D. Wyner, "Capacity and error exponent for the direct detection photon channel-part i-ii," *IEEE Transactions on Information Theory*, vol. 34, no. 6, p. 14491471, 1988.
- [23] K. Chakraborty, S. Dey, and M. Franceschetti, "Outage capacity of mimo poisson fading channels," *IEEE Transactions on Information Theory*, vol. 54, no. 11, pp. 4887–4907, 2008.
- [24] A. Lapidot and S. M. Moser, "On the capacity of the discrete-time poisson channel," *IEEE Transactions on Information Theory*, vol. 55, no. 1, pp. 303–322, 2009.
- [25] C. Gong and Z. Xu, "Channel estimation and signal detection for optical wireless scattering communication with inter-symbol interference," *IEEE Transactions on Wireless Communications*, vol. 14, no. 10, pp. 5326–5337, 2015.
- [26] —, "Non-line of sight optical wireless relaying with the photon counting receiver: A count-and-forward protocol," *IEEE Transactions on Wireless Communications*, vol. 14, no. 1, pp. 376–388, 2015.
- [27] C. Gong, K. Wang, Z. Xu, and X. Wang, "On full-duplex relaying for optical wireless scattering communication with on-off keying modulation," *IEEE Transactions on Wireless Communications*, vol. 17, no. 4, pp. 2525–2538, 2018.
- [28] K. Wang, C. Gong, D. Zou, and Z. Xu, "Turbulence channel modeling and non-parametric estimation for optical wireless scattering communication," *Journal of Lightwave Technology*, vol. 35, no. 13, pp. 2746–2756, 2017.
- [29] D. Zou, C. Gong, K. Wang, and Z. Xu, "Characterization on practical photon counting receiver in optical scattering communication," *IEEE Transactions on Communications*, vol. 67, no. 3, pp. 2203–2217, 2019.
- [30] G. Wang, K. Wang, C. Gong, D. Zou, Z. Jiang, and Z. Xu, "A 1mbps real-time nlos uv scattering communication system with receiver diversity over 1km," *IEEE Photonics Journal*, 02 2018.
- [31] G. Romero, J. J. García-Ripoll, and E. Solano, "Microwave photon detector in circuit qed," *Phys. Rev. Lett.*, vol. 102, p. 173602, 2009.
- [32] C. Eichler, D. Bozyigit, C. Lang, L. Steffen, J. Fink, and A. Wallraff, "Experimental state tomography of itinerant single microwave photons," *Phys. Rev. Lett.*, vol. 106, p. 220503, 2011.
- [33] E. C. G. Sudarshan, "Equivalence of semiclassical and quantum mechanical descriptions of statistical light beams," *Phys. Rev. Lett.*, vol. 10, pp. 277–279, 1963.
- [34] R. J. Glauber, "Coherent and incoherent states of the radiation field," *Phys. Rev.*, vol. 131, pp. 2766–2788, 1963.
- [35] K. HUSIMI, "Some formal properties of the density matrix," *Proceedings of the Physico-Mathematical Society of Japan. 3rd Series*, vol. 22, no. 4, pp. 264–314, 1940.
- [36] E. P. Menzel, F. Deppe, M. Mariani, M. A. Araque Caballero, A. Baust, T. Niemczyk, E. Hoffmann, A. Marx, E. Solano, and R. Gross, "Dual-path state reconstruction scheme for propagating quantum microwaves and detector noise tomography," *Phys. Rev. Lett.*, vol. 105, p. 100401, 2010.
- [37] U. Equipment, "radio transmission and reception (release 12), 3gpp ts 36.101, v12. 13.0, 2016."